Optimizing the Properties of the Protein Corona Surrounding Nanoparticles for Tuning Payload Release

Anna Cifuentes-Rius,[†,§,⊥] Helena de Puig,[‡,⊥] James Chen Yong Kah,[§,∥] Salvador Borros,[†] and Kimberly Hamad-Schifferli[‡,§,¶,*]

[†]Grup d'Enginyeria de Materials (GEMAT), Institut Quimic de Sarrià, Universitat Ramon Llull, Via Augusta 390, 08017 Barcelona, Spain, and [‡]Department of Mechanical Engineering and [§]Department of Biological Engineering, Massachusetts Institute of Technology, Cambridge, Massachusetts 02139, United States. [⊥]These authors contributed equally. [∥]Present address: Nanomedicine & Nanobiology Lab, Department of Biomedical Engineering, National University of Singapore, Singapore 117576. [¶]Present address: MIT Lincoln Laboratory, 244 Wood Street, Lexington, MA 02420.

ABSTRACT

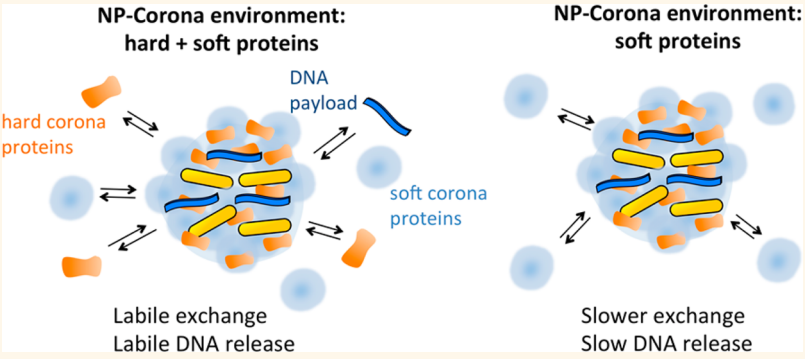

We manipulate the passive release rates of DNA payloads on protein coronas formed around nanoparticles (NPs) by varying the corona composition. The coronas are prepared using a mixture of hard and soft corona proteins. We form coronas around gold nanorods (NRs), nanobones (NBs), and carbon nanotubes (CNTs) from human serum (HS) and find that tuning the amount of human serum albumin (HSA) in the NR-coronas (NR-HS-DNA) changes the payload release profile. The effect of buffer strength, HS concentration, and concentration of the cetyltrimethylammonium bromide (CTAB) passivating the NP surfaces on passive release is explored. We find that corona properties play an important role in passive release, and concentrations of CTAB, HS, and phosphate buffer used in corona formation can tune payload release profiles. These advances in understanding protein corona properties bring us closer toward developing a set of basic design rules that enable their manipulation and optimization for particular biological applications.

KEYWORDS: protein corona · nanorods · nanobones · carbon nanotubes · controlled release DNA

When nanoparticles (NPs) are introduced into biological fluids and systems, the proteins and small molecules that are present adsorb onto the NP surface, forming a protein corona.[1,2] The protein corona is multilayered and held together by numerous noncovalent bonds. Because corona properties are so complex, it is difficult not only to characterize it but also to predict its behavior. Furthermore, the corona physically masks the surface of the NP and can obscure the function of antibodies, ligands, or aptamers directly attached to the NP.[3−5] Despite continued efforts to render NP surfaces nonfouling,[6,7] growing evidence shows that corona formation cannot be avoided.

However, important advances in understanding the protein corona have been made. While the NPs have varied among studies, the key finding is that certain classes of proteins bind strongly to the NPs making up the "hard corona", while others interact more weakly with the NP, forming the "soft corona".[8−10] Once formed, the corona is not static, where its proteins

* Address correspondence to schiffer@mit.edu, kimberly.hamad-schifferli@ll.mit.edu.

Received for review August 9, 2013 and accepted October 7, 2013.

Published online October 15, 2013
10.1021/nn404166q

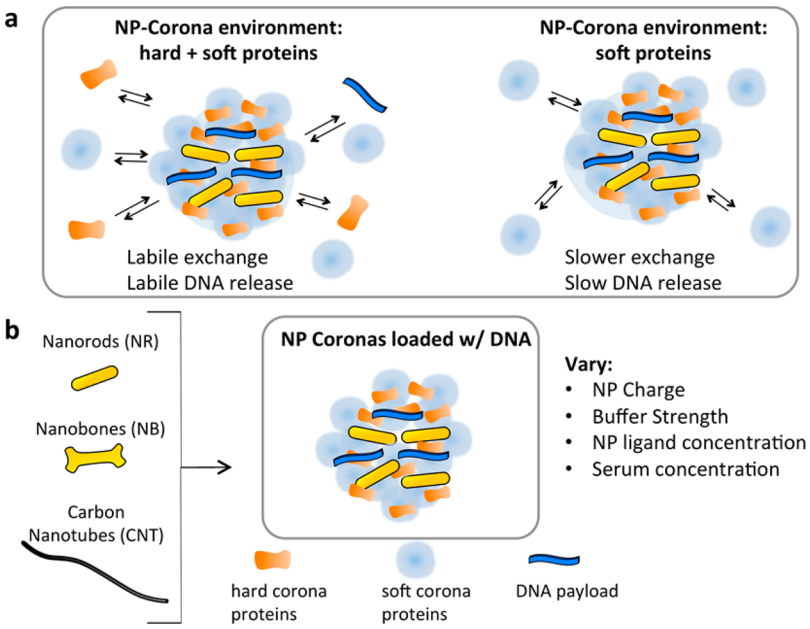

Scheme 1. Graphical representation of the corona design approach. (a) Schematic of the corona exchange concept. NRs with human serum coronas loaded with DNA (NR-HS-DNA) in the presence of hard (orange) and soft (blue) corona proteins experience more labile release and higher release, while in the presence of soft corona, proteins experience slower and lower release of DNA. (b) Formation of HS-DNA conjugates around NRs, NBs, and CNTs. The loading and passive release of a DNA payload is monitored for different NP charge, corona compositions, buffer strengths, and serum concentrations.

are continuously exchanging with free species in the surroundings. These change as the NP moves through different physiological environments, causing the protein corona to evolve.[11−15] These advances in understanding the protein corona properties have brought us closer toward developing basic "design rules" that would enable us to manipulate their properties and optimize them for a particular biological application.

Protein coronas have promising properties that can be exploited.[16] The corona is large and multilayered and can be used to improve carrier properties for drug delivery by holding high amounts of therapeutic payloads. Recently, we demonstrated that protein coronas on gold nanorods (NRs) can be loaded with DNA and doxorubicin at capacities 5−10-fold higher than what is achievable by covalent chemistry.[17] Furthermore, because the protein corona is formed from endogenous proteins, undesirable immune responses to the therapeutic carrier could potentially be minimized or eliminated altogether.[18] Moreover, the presence of proteins on the NP surface could also facilitate transmembrane internalization due to the higher amount of exposed ligands on the corona, which could assist recognition by cell membrane receptors.[19] Thus, NR-coronas are unique carriers with enhanced physical and biological properties and have great promise for improving drug delivery.

However, depending on the delivery application, different modes of payload release may be desirable. Some applications require release at a constant rate to optimize the therapeutic index. In other cases, it is necessary to have no payload release until an external trigger, such as a change in biological or chemical environment, or excitation by an external source.[20] Therefore, guidelines for constructing a protein corona that exhibits a particular release behavior would add further value to its potential as a therapeutic carrier.

Here we build upon these common observations about protein coronas to manipulate and optimize their properties for therapeutic delivery. It is expected that when NPs with protein coronas are in an environment with an abundance of hard corona proteins, exchange will occur between those in the environment and on the NP (Scheme 1a).[14] If the corona on the NP contains a payload, this exchange would induce payload release. However, if only soft corona proteins are present in the environment, the amount of exchange will be limited, resulting in less payload release. Therefore, one can use these two different protein classes to manipulate the exchange and consequently the release profile.

We employ this exchange strategy on NPs of interest to biological applications (NRs, gold nanobones, NBs, and carbon nanotubes, CNTs) with coronas formed from human serum (HS) (Scheme 1b). NRs, NBs, and CNT-coronas were loaded with a DNA oligonucleotide payload, and their release profiles were monitored. We also examined the effect of varying buffer strength, passivating ligand concentration, and HS amount on the passive release of DNA. The robustness of the NR-coronas in changing buffer conditions and blood plasma were explored. We show that we can strategically tune corona properties to either minimize leakage for triggered release applications or to control the rate of constant passive release.

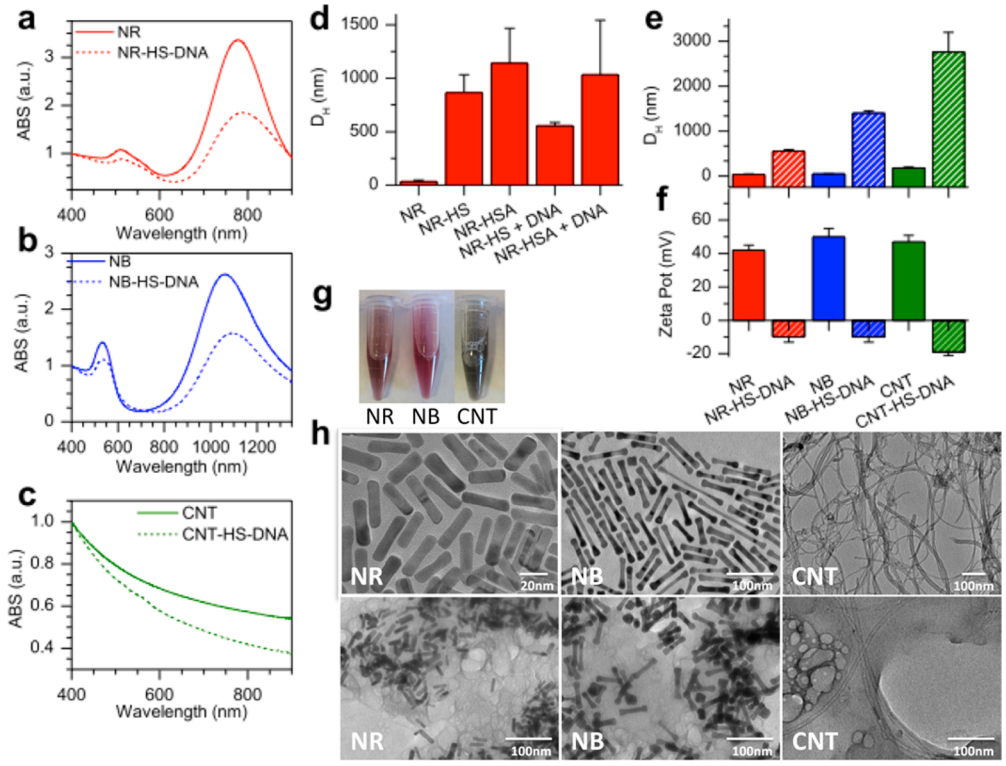

Figure 1. Characterization of NR/NB/CNT-coronas. Absorption spectra of (a) NRs, (b) NBs, and (c) CNTs before (solid line) and after (dashed line) the formation of the protein coronas. (d) Average hydrodynamic diameter, D_H, of the NRs with different corona formation approaches, using human serum (HS) or the pure protein human serum albumin (HSA) as measured using DLS. (e) D_H of particles and coronas made with HS measured by DLS. (f) Zeta-potential of particles and coronas. (g) Image of the vials after corona formation shows that nanoparticles are stable in solution. (h) TEM images of NRs and NR-HS-DNA, NBs and NB-HS-DNA, and CNTs and CNT-HS-DNA.

RESULTS AND DISCUSSION

DNA Loading and Characterization of NP-Coronas. We formed protein coronas on three types of NPs: CTAB-coated gold NRs (40 × 10 nm), NBs (85 × 11 nm), and CNTs (5 μm x 15 nm). Coronas were made from two different protein systems: human serum (HS), which contains a mix of hard and soft corona proteins,[2,14] and pure human serum albumin (HSA), a known soft corona protein that is the major component of HS (which has a HSA concentration of ~6 mg/mL). The corona payload was a 20 base DNA oligo tagged with the fluorophore TAMRA (5′-CAG CGT GCG CCA TCC TTC CC TMR-3′). Coronas were formed around the NRs, NBs, and CNTs using a previously published approach.[17] DNA can be loaded either simultaneously with HS or HSA corona formation on NPs (simultaneous assembly) or after the NP-HS/HSA corona was formed (sequential assembly). Simultaneous assembly was used unless otherwise noted.

Optical characterization of both NR-coronas (NR-HS-DNA) and NB-coronas (NB-HS-DNA) showed that the longitudinal surface plasmon resonance (LSPR) of the NRs was still visible, with a minor red shift and slight broadening over the CTAB-coated NRs (solid *vs* dashed lines, Figure 1a,b, respectively). LSPR red shifts and broadening indicated that the NRs and NBs were in proximity to one another in the corona. Both CNT-coronas (CNT-HS-DNA) and naked CNTs showed absorption spectrum typical of Mie scatterers due to the lack of SPR in CNTs (Figure 1c). DLS (Figure 1d) revealed that when coronas were formed from either HS or HSA, a larger species resulted. NRs had an average D_H = 32 ± 15 nm which increased to D_H = 865 ± 167 nm with HS corona formation or D_H = 1138 ± 330 nm with HSA corona formation. The increase in D_H was also observed for NBs and CNTs (Figure 1e). These size increases suggested that both HS and HSA formed large coronas around a cluster of multiple NPs, and that HSA apparently formed a larger corona than HS. This could be due to the fact that HSA is a soft corona protein, which has a weaker interaction with the NPs. The size increase was not as large for coronas formed with DNA payloads, which could be due to differences in the corona composition or binding strength in the presence of the negatively charged DNA. Even though the NR-coronas contained multiple NRs, the absorption spectrum indicated that the NRs were sufficiently separated not to have their SPRs strongly interact. Zeta-potential measurements of all three positively charged NPs showed that as the NP-coronas were formed, they adopt a similar negative charge (Figure 1f) due to the negative species that dominate HS composition. Furthermore, CNT-HS-DNA, NR-HS-DNA, and NB-HS-DNA exhibited

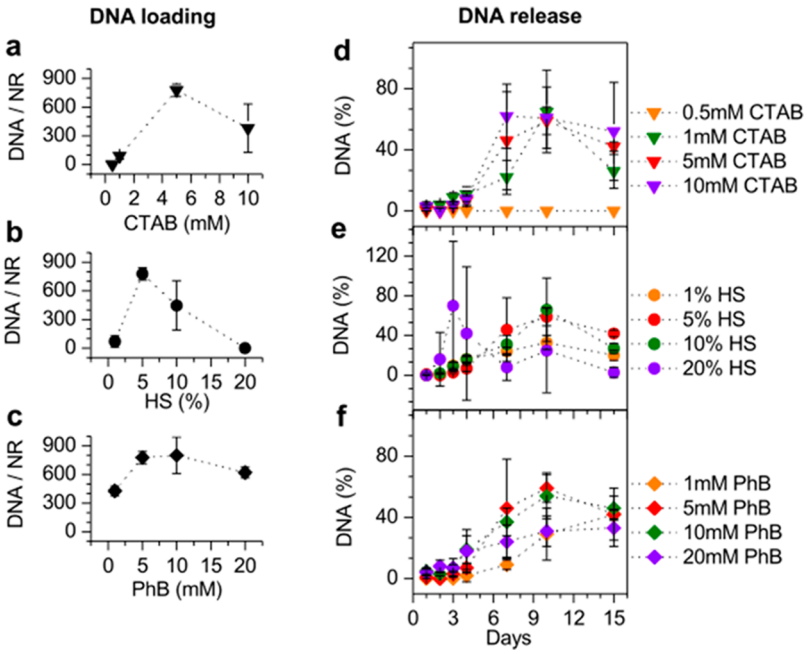

Figure 2. Effect of environmental and assembly conditions on loading and passive release of DNA from NR-HS-DNA. (a) Varying CTAB, (b) HS and (c) phosphate buffer (PhB) concentration during corona assembly and their effect on DNA loading per NR. Effect of varying (d) CTAB, (e) HS, and (f) PhB concentration on DNA passive release profiles.

good colloidal stability in solution after corona formation (Figure 1g).[21] TEM images of all three types of NP-HS-DNA show large, diffuse agglomerates containing many NPs, confirming that there are not one but many NPs in a corona (Figure 1h).

Tuning DNA Loading and Passive Release by Varying Corona Formation Conditions. We varied conditions for corona formation to determine optimal parameters for highest DNA loading on NRs. DNA loading (number of DNA/NR) was measured on the first day of the experiment by heating the sample at 90 °C for 30 min and quantifying the TAMRA-conjugated DNA released in the supernatant.[17] We observed that the DNA loading measured at day 1 is often lower than the amount of DNA passively released after 10 days, which shows that protein corona properties are complicated, and that it is difficult to displace all the DNA from the coronas when they are initially formed.

We examined how the concentration of CTAB affected DNA loading in the corona (Figure 2a). DNA loading was negligible at [CTAB] < 1 mM but increased slightly to 88 ± 33 DNA/NR for [CTAB] = 1 mM. DNA loading peaked at 777 ± 64 DNA/NR at [CTAB] = 5 mM, before decreasing to 380 ± 252 DNA/NR at [CTAB] = 10 mM. Because CTAB binds weakly to the NPs, it is in dynamic flux with the environment, where it switches between bound and unbound states. Due to its charge, CTAB can interact with both the DNA and the negatively charged corona proteins. Excess CTAB can form stable micelles that could interact with the free HS proteins and DNA, thus competing with corona formation and DNA loading on the NP surface. This excess of CTAB will not only have a negative effect on the loading capacities of the formed protein coronas but may also increase the cytotoxicity of these DNA vehicles when used in biological systems.[19] On the other hand, if the CTAB concentration is below its critical micelle concentration, CMC (CMC_{CTAB} = 1.2 mM[22,23]), the NPs are not fully passivated,[24,25] so fewer HS proteins are able to interact with the NPs and form a corona and load DNA. Therefore, CTAB is intimately involved in corona formation, and its concentration affects DNA loading on the NPs.

We probed the effect of varying HS concentration from 1 to 20% during corona formation on the DNA loading (Figure 2b). DNA loading was low for 1% HS (70 ± 58 DNA/NR) and peaked at 777 ± 64 DNA/NR for 5% HS. At higher HS concentrations, the loading decreased (477 ± 259 DNA/NR for 10% HS coronas), becoming negligible at 20% HS. This shows that the concentration of HS used to form the corona also affects the amount of DNA loaded. When large amounts of HS are present, the HS proteins may compete with the DNA for the positively charged surface of the NPs, thus reducing the loading of DNA within the corona. Moreover, the excess of HS may lead to the formation of larger aggregates, as suggested by the red shifts and peak broadening of the LSPR (Supporting Information, Figure S3), which in turn reduces their stability in solution.

Lastly, we varied the phosphate buffer concentration during corona formation and DNA loading (Figure 2c). The DNA loading profile varied with PhB, showing that PhB influences the protein corona integrity and thus its ability to hold payload, which is most likely due to the charge screening modulating the electrostatic

interactions between the DNA, corona proteins, and CTAB. Of all the three parameters, PhB had the weakest effect on corona loading.

Changing [CTAB], HS%, and [PhB] also affected the passive release of DNA (Figure 2d–f and Supporting Information Figure S4a–c). NR-HS-DNA showed low DNA release during the first 4 days for the three concentrations of CTAB that showed non-negligible DNA loading (1, 5, and 10 mM) (Figure 2d). Release increased thereafter, with a large release at day 7, particularly in the presence of 5 and 10 mM CTAB. This initial 3–4 day lag was observed previously for NRs coated with coronas of equine serum.[17] Previous studies have found that the composition of the corona changes during an initial period, before the corona hardens (after ~48 h).[11] This initial lag is beneficial for triggered release experiments, where the corona can be used to hold the payload within the first three days without significant passive release. The amount of DNA passively released increased with [CTAB] (Figure 2d). Varying HS% and [PhB] also affected passive release (Figure 2e,f), and the amount released correlated with the amount of DNA initially loaded. The initial 3–4 day lag was shortened to 2 days for high PhB concentrations (20 mM) and low HS concentrations (1%), indicating that the ability of the protein corona to hold onto the DNA payloads at earlier time points is also dependent on the protein and ionic environment.

Evolution of Protein Corona Affects Passive Release. The coronas around NPs are known to change in different environments. We explored the effect of making NR-HS-DNA coronas at one ionic strength and then introducing them to a solution with a different ionic strength (Figure 3 and Supporting Information Figure S5). NR-HS-DNA was formed in [PhB] = 5 mM, and then release profiles were measured in [PhB] = 1, 5, and 10 mM. We observed that the coronas formed at 5 mM PhB and then introduced to 1 mM PhB (Figure 3a, blue diamonds) have a passive release profile that is different from the coronas formed and released at 5 mM PhB (Figure 3a, red diamonds) and those formed and released at 1 mM PhB (Figure 3a, orange diamonds). Similarly, the NR-HS-DNA formed at 5 mM PhB and released at 10 mM PhB (Figure 3b, purple diamonds) also show a different release profile between that formed and released at 10 mM PhB (Figure 3b, green diamonds) and that formed and released at 5 mM PhB (Figure 3b, red diamonds). Both release profiles in 1 mM and 10 mM PhB showed the same initial 3 day lag as that of coronas made and released in 5 mM, indicating that when the coronas are formed in one PhB concentration and then used for release in another, the release profile retains some of its original release properties, resulting in an intermediate behavior. Thus, the corona has some resilience that can be maintained in different buffer solutions for several days.

HS and HSA Make Coronas with Different Capacities for DNA Loading. While both HS and HSA can form a corona

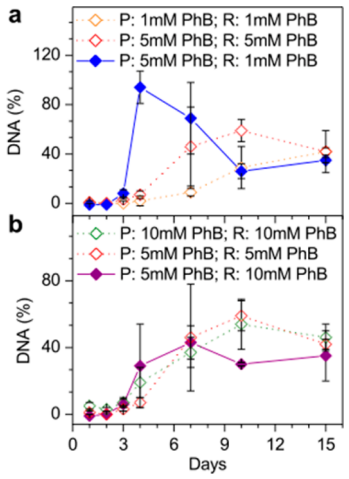

Figure 3. Effect of forming NR-HS-DNA in one PhB concentration, and measuring the passive release in a different PhB concentration. (a) NR-HS-DNA were prepared (P) in [PhB] = 5 mM using 5% HS, and then passive release (R) measured in 5 mM (red diamonds) and 1 mM (blue diamonds). NR-HS-DNA prepared in [PhB] = 1 mM and a passive release profile measured in 1 mM (orange diamonds). (b) NR-HS-DNA prepared in 5 mM PhB and released in 10 mM PhB (purple diamonds) and 5 mM PhB (red diamonds). NR-HS-DNA formed in 10 mM PhB and released in 10 mM PhB (green diamonds) for comparison.

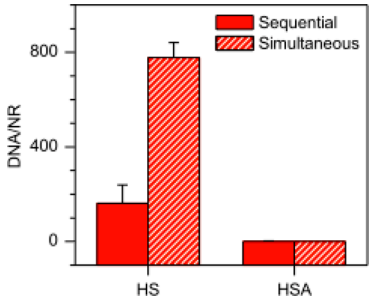

Figure 4. HS and HSA form different types of coronas. DNA loading for NR-HS *vs* NR-HSA formed by sequential (solid) and simultaneous (hashed) assembly.

around NPs, their ability to carry a DNA payload differs. NR-HS coronas can be loaded with 162 ± 78 to 777 ± 64 DNA/NR depending on the assembly approach (Figure 4), a payload capacity similar to NRs with coronas made of equine serum.[17] In contrast, NR-HSA coronas had negligible DNA loading for both assembly approaches, ~0 DNA/NR. Although a corona was formed from HSA, as evidenced by the increase in D_H (Figure 1e), it was not as effective as HS at loading DNA. This is most likely due to the fact that HSA is a soft corona protein, which forms a larger and more loosely bound corona and does not interact strongly with DNA. Based on these results, it appears that components in the HS other than HSA are responsible for holding the NR, corona, and DNA payload together.

Despite its poor loading capacity, HSA can potentially function as a blocking agent for NR-HS-DNA, where it could be used to form an additional corona layer around already formed coronas to block passive

DNA release on already-formed coronas. Because HSA is a soft corona protein, it has limited exchange with the hard corona proteins in HS and consequently results in slower release of DNA from the corona (Scheme 1b). This property can be exploited to hold the payload in the corona for an extended period of time prior to their triggered release. In contrast, HS contains hard corona proteins that can exchange with those in the NR-HS-DNA to promote payload release. Therefore, a rational selection of protein environment could provide us with a handle for manipulating the payload release profile.

Exploiting Corona Exchange for Manipulating Payload Release. Extending the idea that HS an HSA have different capacities to form payload-carrying coronas, we tested the ability of the protein environment to manipulate the passive release of DNA from NR-HS-DNA. We compared passive release of DNA from NR-HS-DNA whose corona was exchanged with HS or HSA. Corona exchange was achieved by placing NR-HS-DNA in a solution of HS or HSA, and release was quantified by measuring the DNA in the supernatant as a function of time. Release was compared to NR-HS-DNA that were not exchanged with HS or HSA ("no block").

The release profile changed depending on the protein environment (Figure 5 and Supporting Information Figure S6). If the NR-coronas were placed in 0.15% soft corona proteins (HSA), less DNA was released (Figure 5a, red triangles) compared to the control without corona exchange (Figure 5a, red squares). HSA was thus able to reduce the passive release of DNA from the NR-HS-DNA, most likely by minimizing the protein exchange in the corona. However, when corona exchange was performed in 0.15% HS, a burst of payload release occurred during the first 4 days (Figure 4a, red circles). In fact, ~20% (264 ± 83 DNA/NR) of payload was already passively released at day 1, whereas the same amount of release is not reached until day 7 for the HSA exchange. This is most likely due to significant protein exchange occurring between the free HS proteins and those in the corona, supporting our postulation that other components in HS other than HSA are perturbing the corona to release more payload. The responsible protein components are most likely the hard corona proteins in the HS that are able to exchange with the existing corona proteins on the NR because of similar binding affinity. Therefore, an appropriate selection of blocking proteins can provide a means to control payload release rate.

Corona Loading and Exchange on Different Nanoparticles. We investigated whether this exchange phenomenon could also be applied to NBs and CNTs, which are also used for drug delivery and release applications.[26−28] NB-HS-DNA had 710 ± 130 DNA/NB (Figure 5e) and a surface loading density of 0.2 DNA/nm^2. This is lower compared to NRs (777 ± 64 DNA/NR, 1 DNA/nm^2) (Figure 5d). CNT-HS-DNA had 1.2 × 10^6 ± 0.62 × 10^6

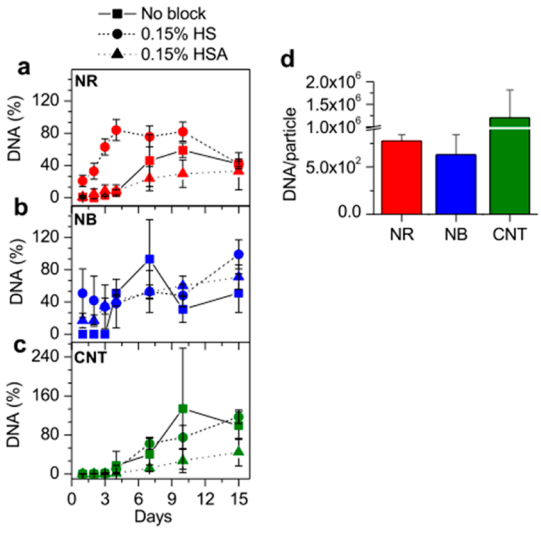

Figure 5. DNA release from coronas with different exchange conditions. Passive release DNA profiles of coronas in an exchange environment of 0.15% HS (circles), 0.15% HSA (triangles), or no protein (squares) on (a) NRs, (b) NBs, and (c) CNTs. Coronas were made using 5% HS in 5 mM PhB for the experiments. (d) DNA loadings on NRs, NBs, and CNTs with no blocking.

DNA/CNT (Figure 5d) and a loading density of 7 DNA/nm^2, which is much higher than the amount achieved for both NRs and NBs (Figure 5d). These results show that coronas can be formed and loaded with DNA on different NPs, although their loading densities differed.

NB-HS-DNA without corona exchange passively released DNA with a profile similar to the NRs, starting with negligible release in the first 3 days and then increasing with time (Figure 5b, blue squares). However, corona exchange with 0.15% HSA seemed to increase the amount of DNA passively released at the beginning (354 ± 218 DNA/NB or 17 ± 9% of initially loaded DNA at day 1) (Figure 5b, blue triangles). This amount is even higher (848 ± 279 DNA/NB or 51 ± 30% of loaded DNA) in the presence of 0.15% HS (Figure 5b, blue circles). Apparently, coronas formed on larger NBs are more prone to leakage, and HSA seems less effective in blocking passive release compared to NRs. As was previously reported, NP size can also influence corona formation.[2,29,30] While blocking was not observed with 0.15% HSA compared to the control in NBs, we were still nonetheless able to demonstrate differential passive release between HS and HSA as with NRs.

CNT-HS-DNA also exhibited the same initial 3 day lag in the passive release of DNA for all three cases (control, corona exchange with HSA, and corona exchange with HS), after which the release increased significantly (Figure 5c). After 3 days, the released concentration of DNA was lowest with HSA blocking (Figure 5c, green triangles), reaching only 45 ± 28% of the loading at day 15, and highest after corona exchange with HS (Figure 5c, green circles), similar to

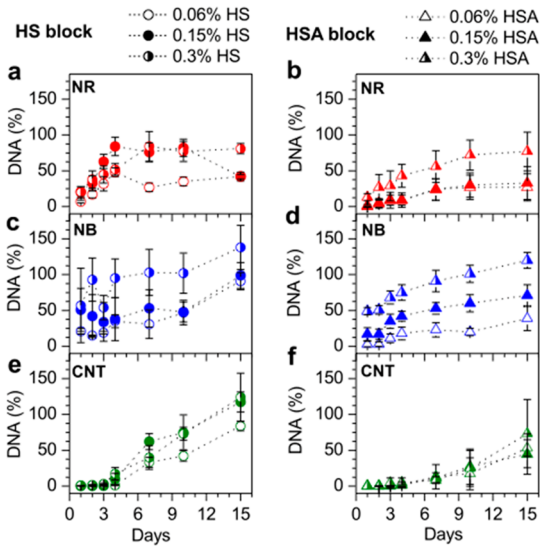

Figure 6. Passive release of DNA from coronas by varying the amount of HS and HSA exchange. Coronas blocked with 0.06, 0.15, and 0.3% HS on (a) NRs, (b) NBs, and (c) CNTs. Coronas blocked with 0.06, 0.15, and 0.3% HSA on (c) NRs, (d) NBs, and (e) CNTs.

the observations for NRs. These results suggest that, apart from size, the amount of CTAB passivation plays a dominant role in influencing corona formation, loading, and release. Since the concentration of CTAB passivating each of the NPs differs due to surface chemistry and available surface area, this could be responsible for the differences in loading, blocking, and exchange dynamics and consequently passive release behavior.

Tuning Payload Release by Changing Protein Concentration in Corona Exchange. We examined the effect of varying the HS and HSA concentration in blocking to tune passive release (Figure 6 and Supporting Information Figure S7). Increasing the HS% used for corona exchange increased the DNA released from the NRs (Figure 6a). A similar trend was observed for increasing the HSA% (Figure 6b), although the release amounts were lower, confirming that HSA is better at blocking the coronas than HS. Evidently, a higher protein concentration in the NR-HS-DNA environment facilitates a greater degree of exchange, thus inducing a larger amount of DNA released. Similar behavior was also observed for NBs and CNTs (Figure 6c–f).

Leakage in Blood Plasma. We investigated passive release of DNA from NR-HS-DNA in human blood plasma, which contains both hard and soft corona proteins (Figure 7 and Supporting Information Figure S8). We measured profiles of passively released DNA from 1.5 nM of NR-HS-DNA with and without blocking with 0.3% HSA. In the absence of blocking, 369 ± 89 DNA was loaded per NR, out of which 58 DNA/NR (15.7% of loaded DNA) was released at day 1 after preparation (Figure 7, orange squares). The amount of released DNA remained relatively constant until day 15,

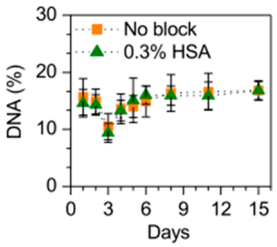

Figure 7. Leakage of DNA in blood plasma from NR-HS-DNA with no blocking (orange squares) and NR-HS-DNA in blood plasma blocked by 0.3% HSA (green triangles).

and no initial lag was observed. This shows that as soon as the NR-HS-DNA is placed into plasma, a small amount of DNA is released, probably due to the exchange with hard corona proteins in the plasma. Released DNA decreased slightly at 3 days, perhaps due to the corona reorganization, where DNA loads back onto the NR-HS-DNA as the blood plasma proteins contributed to the existing corona.

The DNA release profile was similar for NR-HS-DNA blocked by 0.3% HSA. In this case, 130 ± 37 DNA was loaded per NR, of which 19 DNA/NR was released at day 1 (Figure 7b, green triangles). Although the amount of DNA released was much lower, the percentage of loaded DNA that was released on day 1 (14.6% of loaded DNA) is only slightly lower compared to that without blocking. This shows that blocking can decrease the concentration of passively released DNA.

In practice, effective blocking by HSA may be difficult to achieve since the blood plasma contains a large number of hard and soft corona proteins that can easily exchange with the corona on the NRs, including the HSA used for blocking. This is evident from the similar dip at day 3 for this experiment, suggesting that corona reorganization could also be taking place with the 0.3% HSA present. However, in both cases, we observed no further increase in the DNA leakage beyond day 8. This shows that the protein corona can be used to hold the loaded DNA stably for more than a week in blood.

CONCLUSIONS

These results show that it is possible to tune the passive release profile of protein coronas by varying the corona composition and NP surface properties. By exploiting the fact that hard and soft corona proteins have different exchange rates, strategic exposure to hard or soft corona proteins can tune the rate of release of a DNA payload from NPs. Hard corona proteins exchange more and result in higher release, while soft corona proteins cause a lower degree of exchange and can be used to decrease passive release. By adsorbing HSA onto already-formed NP-HS-DNA coronas, DNA release rate can be slowed. This strategy can be employed on different types of NPs

and is easily extended to other NPs with similar ligands. These results can aid the manipulation of corona properties to optimize them for biological applications.

MATERIALS AND METHODS

Gold Nanorod and Nanobone Synthesis. Gold NRs and NBs were synthesized by standard seed and non-seed-mediated methods from the literature.[31] For the synthesis of gold nanorods, a single surfactant non-seed-mediated growth method in 20 mL batches was used. Then, 240 μL of 50 mM gold chloride trihydrate ($HAuCl_4$) was added to 16.67 mL of 0.2 M cetyltrimethylammonium bromide (CTAB) mixed with 300 μL of 100 mM sodium chloride (NaCl), and the solution turned orange; 240 μL of 10 mM silver nitrate ($AgNO_3$) was added to the solution, followed by gentle mixing; 200 μL of 100 mM ascorbic acid (AA) was added, followed by inversion until the solution turned colorless. Finally, 128 μL of 0.3125 mM sodium borohydride ($NaBH_4$) was added. The solution sat on the bench undisturbed overnight at room temperature, during which time it turned reddish brown, indicating the presence of NRs. Transmission electron microscopy (TEM) analysis showed that the NRs had dimensions of 35 ± 5 nm $\times$ 10 ± 1 nm.

Gold nanobones were synthesized by a binary surfactant seed-mediated growth method. First, gold seeds were prepared by mixing 7.5 mL of 0.2 M CTAB with 2.5 mL of 1 mM $HAuCl_4$ and 0.6 mL of ice-cold 0.01 M $NaBH_4$. After, the growth solution was prepared by adding 25 mL of 1 mM $HAuCl_4$ and 1 mL of 4 mM $AgNO_3$ into a mixture of 10 mL of 0.2 M CTAB and 15 mL of 0.3 M benzyldimethylhexadecylammonium chloride (BDAC), and the solution turned orange. Then, 0.3 mL of 0.1 M ascorbic acid was added to the solution, followed by gentle mixing until the solution turned colorless. Finally, 0.05 mL of the seed solution was added to the growth solution. The solution was sat undisturbed overnight and turned reddish-purple, forming long gold nanocapsules. The day after the synthesis, 1 mL of 0.1 M ascorbic acid was added to every 50 mL of long nanocapsule solution, turning them into nanobones. TEM imaging showed that the NBs have dimensions of 85 ± 14 $\times$ 11 ± 2. All the reagents were purchased from Sigma-Aldrich, except for NaCl, which was from Mallinckrodt.

After the synthesis, NRs and NBs were washed to remove the excess reagents (30 min at 13 500 rcf) resuspended in Milli-Q water and stored until usage. NPs were centrifuged twice in the desired concentration of CTAB (from 0.5 to 10 mM, but typically 5 mM) before proceeding to the corona formation.

Carbon Nanotube Solubilization and Characterization. Carbon nanotubes (CNTs) were purchased from NanoLab Inc. and were dispersed with CTAB. Highly well-dispersed CNT-CTAB was obtained after dissolving the CNT in 5 mM CTAB (2 mg/mL), followed by sonication (2 h) and centrifugation (16 200 rcf, 1 h) to isolate the highly dispersed carbon nanotubes from the bundles. A set of dispersions (from 2.5 to 40 μg/mL) was prepared by diluting the original dispersion (CNT-CTAB 2 mg/mL) with 5 mM CTAB. These dispersions were sonicated for 30 min before UV–vis analysis. The absorption at 500 nm was used to determine the concentration of the final well-dispersed CNTs. Knowing that the purchased CNTs were 1–5 μm length, 15 ± 5 diameter, and 2.1 g/mL density average, the concentration obtained was converted to nanomolar. CNT-CTAB conjugates were washed with Milli-Q water by using centrifuge filters (Amicon Ultra-0.5 mL, Merck Millipore).

Corona Formation. Human serum (HS) and human serum albumin (HSA) were purchased from Sigma-Aldrich. The DNA used had a sequence of 5′-CAG CGT GCG CCATCC TTC CC-TMR-3′ (BCL2, MW = 6998.8, Integrated DNA Technologies, Inc.).

The corona formation was carried out *via* sequential and combined method. Both needed a previous centrifugation (13 500 rcf for 30 min) of 1 mL of washed nanoparticles (either gold nanorods, gold nanobones, or carbon nanotubes; NR/NB/CNT). The obtained pellet was resuspended with the corona cocktail.

In the sequential method, the pellet was first resuspended with 500 μL of HS or HSA (5% (v/v) unless otherwise indicated) in 1–20 mM phosphate buffer (PhB, pH 7.4), incubated at 37 °C for 6 h, centrifuged at 4500 rcf for 20 min, and resuspended with 500 μL of 1 μM DNA in PhB.

For the combined assembly, the corona cocktail was previously prepared together (protein and DNA) with same final concentrations as described before (500 μL of 1 μM DNA and 5% HS in PhB) which was used to resuspend the pellet. All nanoparticles were incubated overnight at 37 °C to enable DNA loading and, after incubation, were washed twice with 500 μL of PhB.

Blocking of the Formed Corona. In the blocking process, the last wash during the corona formation was carried out with 500 μL of HS or HSA solution (0.06, 0.15, and 0.3% (v/v)) in 5 mM PhB.

Nanoparticle and Corona Characterization. Both naked NPs and the corona conjugates were analyzed by UV–vis spectrophotometry. For NRs and CNTs, the scan carried out was from 400 to 900 nm (Cary 100 UV–vis spectrophotometer, Agilent Technologies), while for the NBs, it was from 400 to 1100 nm (Cary 500i UV–vis–NIR spectrophotometer, Agilent Technologies). NR and NB concentrations of all samples could be determined from the obtained UV–vis spectra and known extinction coefficients. CNT concentration was calculated from the calibration curve, as explained previously.

Alteration of the nanoparticles' morphology when the corona was formed was characterized by TEM. Changes in size and charge were also determined by using dynamic light scattering (DLS, DynaPro Titan, Wyatt Technology Corporation) and zeta-potential (Malvern Zetasizer Nano ZS90).

DNA Loading by Fluorescence. Each sample was thermally treated in order to quantify the DNA initially loaded on the formed NP-coronas. In order to do that, 30 μL aliquots of the NP-coronas were heated at 90 °C for 30 min and centrifuged at 13 500 rcf. The concentration of DNA in the supernatants was quantified by fluorescence spectroscopy of the TMR tag (λ_{ex} = 557 nm and λ_{em} = 581 nm) attached on the 5′ end of the DNA. The same process but without heating was carried out for other 30 μL aliquots of each sample as a control.

Passive DNA Release Profiles. Passively released DNA was measured by quantifying the DNA in the supernatant after a certain period of time. Samples were left at room temperature for 15 days, and at every time point, an aliquot (30 μL) was extracted. The aliquots were centrifuged at 13 500 rcf for 12 min, and the supernatant was diluted in PhB for fluorescence spectroscopy analysis. The leaking percentage was obtained by dividing the passively released concentration of DNA by the loading measured after the thermal treatment (90 °C during 30 min) on day 1.

Passive DNA Release in Blood Plasma. The NR-HS-DNA was prepared with 5% (v/v) HS and 1 μM DNA as detailed previously. Following the formation of the DNA-loaded corona, the NR-HS-DNA was washed twice by centrifugation at 4500 rcf for 20 min in 5 mM PhB prior to blocking by 0.3% HSA in 5 mM PhB. The blocking was performed under 1 h incubation at 37 °C before centrifuging the NR-HS-DNA at 5000 rcf for 20 min and resuspending them in 1 mL of human blood plasma. The blood plasma was obtained from whole human blood (Research Blood Components) by centrifugation at 4500 rcf for 20 min. The NR-HS-DNA was kept in blood plasma at 37 °C over a period of 15 days, during which 100 μL was aliquoted at fixed time points to quantify for the amount of DNA released.

Conflict of Interest: The authors declare no competing financial interest.

Acknowledgment. We would like to thank Prof. Lee Gehrke for experimental support (Harvard-MIT HST/IMES), the Bawendi group, the MIT CMSE for use of the experimental facilities, Zhichuan Xu for TEM imaging, the Van Vliet group, the MIT-IQS exchange program, and the MIT-Spain MISTI program. This work was supported by the NSF (DMR #0906838). A.C.R. was supported by MIT-MISTI Spain Program and by an IQS Fellowship. H.dP. was

supported by La Caixa Fellowship. J.C.Y.K. was supported by an NUS Fellowship, and S. B. was supported by the Ministerio de Ciencia y Competividad of Spain for the project SAF2012-39947-C02-0.

Supporting Information Available: DNA loadings, release, and UV–vis spectra. This material is available free of charge *via* the Internet at http://pubs.acs.org.

REFERENCES AND NOTES

1. Walczyk, D.; Bombelli, F. B.; Monopoli, M. P.; Lynch, I.; Dawson, K. A. What the Cell "Sees" in Bionanoscience. *J. Am. Chem. Soc.* **2010**, *132*, 5761–5768.
2. Walkey, C. D.; Olsen, J. B.; Guo, H.; Emili, A.; Chan, W. C. W. Nanoparticle Size and Surface Chemistry Determine Serum Protein Adsorption and Macrophage Uptake. *J. Am. Chem. Soc.* **2012**, *134*, 2139–2147.
3. Salvati, A.; Pitek, A. S.; Monopoli, M. P.; Prapainop, K.; Bombelli, F. B.; Hristov, D. R.; Kelly, P. M.; Aberg, C.; Mahon, E.; Dawson, K. A. Transferrin-Functionalized Nanoparticles Lose Their Targeting Capabilities When a Biomolecule Corona Adsorbs on the Surface. *Nat. Nanotechnol.* **2013**, *8*, 137–143.
4. Mirshafiee, V.; Mahmoudi, M.; Lou, K.; Cheng, J.; Kraft, M. Protein Corona Significantly Reduces Active Targeting Yield. *Chem. Commun.* **2013**, *49*, 2557–2559.
5. Cavadas, M.; González-Fernández, Á.; Franco, R. Pathogen-Mimetic Stealth Nanocarriers for Drug Delivery: A Future Possibility. *Nanomedicine* **2011**, *7*, 730–743.
6. Walkey, C. D.; Chan, W. C. W. Understanding and Controlling the Interaction of Nanomaterials with Proteins in a Physiological Environment. *Chem. Soc. Rev.* **2012**, *41*, 2780–2799.
7. Mahon, E.; Hristov, D. R.; Dawson, K. A. Stabilising Fluorescent Silica Nanoparticles against Dissolution Effects for Biological Studies. *Chem. Commun.* **2012**, *48*, 7970–7972.
8. Monopoli, M. P.; Walczyk, D.; Campbell, A.; Elia, G.; Lynch, I.; Baldelli Bombelli, F.; Dawson, K. A. Physical-Chemical Aspects of Protein Corona: Relevance to *In Vitro* and *In Vivo* Biological Impacts of Nanoparticles. *J. Am. Chem. Soc.* **2011**, *133*, 2525–2534.
9. Liu, W.; Rose, J.; Plantevin, S.; Auffan, M.; Bottero, J.; Vidaud, C. Protein Corona Formation for Nanomaterials and Proteins of a Similar Size: Hard or Soft Corona? *Nanoscale* **2013**, *5*, 1658–1668.
10. Milani, S.; Baldelli Bombelli, F.; Pitek, A.; Dawson, K.; Radler, J. Reversible *versus* Irreversible Binding of Transferrin to Polystyrene Nanoparticles: Soft and Hard Corona. *ACS Nano* **2012**, *6*, 2532–2541.
11. Casals, E.; Pfaller, T.; Duschl, A.; Oostingh, G. J.; Puntes, V. Time Evolution of the Nanoparticle Protein Corona. *ACS Nano* **2010**, *4*, 3623–3632.
12. Arvizo, R. R.; Giri, K.; Moyano, D.; Miranda, O. R.; Madden, B.; McCormick, D. J.; Bhattacharya, R.; Rotello, V. M.; Kocher, J.-P.; Mukherjee, P. Identifying New Therapeutic Targets *via* Modulation of Protein Corona Formation by Engineered Nanoparticles. *PLoS One* **2012**, *7*, e33650.
13. Dell'Orco, D.; Lundqvist, M.; Oslakovic, C.; Cedervall, T.; Linse, S. Modeling the Time Evolution of the Nanoparticle-Protein Corona in a Body Fluid. *PLoS One* **2010**, *5*, e10949.
14. Lundqvist, M.; Stigler, J.; Cedervall, T.; Berggård, T.; Flanagan, M. B.; Lynch, I.; Elia, G.; Dawson, K. The Evolution of the Protein Corona around Nanoparticles: A Test Study. *ACS Nano* **2011**, *5*, 7503–7509.
15. Wang, F.; Yu, L.; Monopoli, M. P.; Sandin, P.; Mahon, E.; Salvati, A.; Dawson, K. A. The Biomolecular Corona is Retained during Nanoparticle Uptake and Protects the Cells from the Damage Induced by Cationic Nanoparticles until Degraded in the Lysosomes. *Nanomedicine* **2013**, in press.
16. Prapainop, K.; Witter, D. P.; Wentworth, P. A Chemical Approach for Cell-Specific Targeting of Nanomaterials: Small-Molecule-Initiated Misfolding of Nanoparticle Corona Proteins. *J. Am. Chem. Soc.* **2012**, *134*, 4100–4103.
17. Kah, J. C. Y.; Chen, J.; Zubieta, A.; Hamad-Schifferli, K. Exploiting the Protein Corona around Gold Nanorods for Loading and Triggered Release. *ACS Nano* **2012**, *6*, 6730–6740.
18. Ge, C.; Du, J.; Zhao, L.; Wang, L.; Liu, Y.; Li, D.; Yang, Y.; Zhou, R.; Zhao, Y.; Chai, Z.; *et al.* Binding of Blood Proteins to Carbon Nanotubes Reduces Cytotoxicity. *Proc. Natl. Acad. Sci. U.S.A.* **2011**, *108*, 16968–16973.
19. Qiu, Y.; Liu, Y.; Wang, L.; Xu, L.; Bai, R.; Ji, Y.; Wu, X.; Zhao, Y.; Li, Y.; Chen, C. Surface Chemistry and Aspect Ratio Mediated Cellular Uptake of Au Nanorods. *Biomaterials* **2010**, *31*, 7606–7619.
20. de Puig, H.; Cifuentes Rius, A.; Flemister, D.; Baxamusa, S. H.; Hamad-Schifferli, K. Selective Light-Triggered Release of DNA from Gold Nanorods Switches Blood Clotting on and off. *PLoS One* **2013**, *8*, e68511.
21. Afrooz, A. R. M. N.; Sivalapalan, S. T.; Murphy, C. J.; Hussain, S. M.; Schlager, J. J.; Saleh, N. B. Spheres *vs.* Rods: The Shape of Gold Nanoparticles Influences Aggregation and Deposition Behavior. *Chemosphere* **2013**, *91*, 93–98.
22. Bahri, M. A.; Hoebeke, M.; Grammenos, A.; Delanaye, L.; Vandewalle, N.; Seret, A. Investigation of SDS, DTAB and CTAB Micelle Microviscosities by Electron Spin Resonance. *Colloids Surf., A* **2006**, *290*, 206–212.
23. Majhi, P. R.; Moulik, S. P. Energetics of Micellization: Reassessment by a High-Sensitivity Titration Microcalorimeter. *Langmuir* **1998**, *14*, 3986–3990.
24. Alper, J.; Crespo, M.; Hamad-Schifferli, K. Release Mechanism of Octadecyl Rhodamine B Chloride from Au Nanorods by Ultrafast Laser Pulses. *J. Phys. Chem. C* **2009**, *113*, 5967–5973.
25. Kah, J.; Zubieta, A.; Saavedra, R.; Hamad-Schifferli, K. Stability of Gold Nanorods Passivated with Amphiphilic Ligands. *Langmuir* **2012**, *28*, 8834–8844.
26. Wijaya, A.; Schaffer, S.; Pallares, I.; Hamad-Schifferli, K. Selective Release of Multiple DNA Oligonucleotides from Gold Nanorods. *ACS Nano* **2009**, *3*, 80–86.
27. Klumpp, C.; Kostarelos, K.; Prato, M.; Bianco, A. Functionalized Carbon Nanotubes as Emerging Nanovectors for the Delivery of Therapeutics. *Biochim. Biophys. Acta* **2006**, *1758*, 404–412.
28. Shannahan, J. H.; Brown, J. M.; Chen, R.; Ke, P. C.; Lai, X.; Mitra, S.; Witzmann, F. A. Comparison of Nanotube–Protein Corona Composition in Cell Culture Media. *Small* **2013**, *9*, 2171–2181.
29. Lundqvist, M.; Stigler, J.; Elia, G.; Lynch, I.; Cedervall, T.; Dawson, K. A. Nanoparticle Size and Surface Properties Determine the Protein Corona with Possible Implications for Biological Impacts. *Proc. Natl. Acad. Sci. U.S.A.* **2008**, *105*, 14265–14270.
30. Tenzer, S.; Docter, D.; Rosfa, S.; Wlodarski, A.; Kuharev, J.; Rekik, A.; Knauer, S. K.; Bantz, C.; Nawroth, T.; Bier, C.; *et al.* Nanoparticle Size Is a Critical Physicochemical Determinant of the Human Blood Plasma Corona: A Comprehensive Quantitative Proteomic Analysis. *ACS Nano* **2011**, *5*, 7155–7167.
31. Sau, T. K.; Murphy, C. J. Seeded High Yield Synthesis of Short Au Nanorods in Aqueous Solution. *Langmuir* **2004**, *20*, 6414–6420.